Revista Colombiana de Estadística
Special Issue: Colombian and Brazil Graduate Programs
December 2025, volume 48, issue 3, pp. 573–587
http://doi.org/10.15446/rce.v48n3.123209

On the Convergence of Expansions for the Exponentiated Transmuted-G Family

Sobre la convergencia de las expansiones en serie para la familia de distribuciones G-transmutada exponenciada

Fernando A. Peña-Ramírez [1,2,a], Renata R. Guerra[1,2,b], Alexsandro A. Ferreira[1,c], Gauss M. Cordeiro[3,d]

[1]Department of Statistics, Centro de Ciências Naturais e Exatas, Universidade Federal de Santa Maria, Santa Maria, Brazil

[2]Graduate Program in Mathematics, Centro de Ciências Naturais e Exatas, Universidade Federal de Santa Maria, Santa Maria, Brazil

[3]Department of Statistics, Centro de Ciências Exatas e da Natureza, Universidade Federal de Pernambuco, Recife, brazil

Abstract

The exponentiated transmuted-G family was introduced along with some of its statistical properties derived from a power series expansion. This work demonstrates that the previously proposed expansions, which depend on a double sum, present convergence problems for some combinations of parameters. Therefore, a much simpler linear representation that depends only on a single sum is presented, allowing for the precise and general calculation of these properties.

***Keywords*:** Exponentiated transmuted-G family; Moments; Power series expansions; Weibull distribution.

Resumen

La familia de distribuciones G-transmutada exponenciada fue introducida junto con algunas de sus propiedades estadísticas derivadas de una expansión en series de potencias. Este trabajo demuestra que las expansiones previamente propuestas, que dependen de una suma doble, presentan problemas de convergencia para algunas combinaciones de parámetros. Por lo tanto, se presenta una representación lineal mucho más simple, que depende solo

[a]Ph.D. E-mail: fernando.p.ramirez@ufsm.br
[b]Ph.D. E-mail: renata.r.guerra@ufsm.br
[c]Ph.D. E-mail: alexsandro.ferreira@acad.ufsm.br
[d]Ph.D. E-mail: gauss@de.ufpe.br

de una suma simple, lo que permite el cálculo preciso y general de estas propiedades.

***Palabras clave*:** Distribución de Weibull; Expansiones en series de potencias; Familia G-transmutada exponenciada; Momentos.

1. Introduction

The development of flexible probability distributions has been a central concern in statistical theory and practice for over a century. The fundamental principle of distribution generalization emerged from the work of Lehmann (1953), who demonstrated that applying a power transformation to a cumulative distribution function yields a new family with enhanced flexibility. This seminal contribution established the theoretical foundation for numerous subsequent extensions. Building upon Lehmann's framework, Gupta et al. (1998) introduced the exponentiated-G (exp-G) family, which generalizes the exponentiation principle to an arbitrary baseline distribution $G(x)$. This family has proven remarkably useful in reliability engineering and survival analysis, enabling practitioners to model complex failure time distributions through a simple power transformation of baseline distributions (Eugene et al., 2002; Cordeiro & de Castro, 2011).

In recent years, several notable advances have further expanded this literature, giving rise to a wide variety of novel and flexible distributions. For example, Cogo et al. (2024) combined the error function generalized family with the Weibull baseline, and Ferreira & Cordeiro (2024) pioneered the flexible generalized gamma distribution, yielding extended models capable of capturing diverse hazard rate shapes. Advances have also been made in the context of discrete distributions. For instance, Debastiani Neto et al. (2025) introduced the discrete xLindley distribution. Moreover, Mota et al. (2021) investigated the reparameterized weighted Lindley distribution, highlighting its tractability and interpretability in modeling discrete data.

Within this general framework, Shaw & Buckley (2007) introduced the transmuted-G (T-G) family through rank transmutation maps, providing an alternative mechanism for generating flexible distributions. This framework has demonstrated substantial utility in modeling diverse phenomena, from reliability data to biomedical applications (Khan & King, 2013; Aryal & Tsokos, 2011). In subsequent work, several authors explored the T-G framework by considering diverse baseline choices such as the Singh–Maddala (Shahzad et al., 2017), Rayleigh (Dey et al., 2017), inverse unit Teissier (Bashiru et al., 2025) and Burr X (Alrweili, 2025) distributions.

The exponentiated transmuted-G (ET-G) family, introduced by Merovci et al. (2017), extends the exp-G and T-G families. Its cumulative distribution function (cdf) is given by

$$F(x) = F(x; \phi, \lambda, \boldsymbol{\xi}) = G(x)^{\phi} \left[1 + \lambda - \lambda\, G(x)\right]^{\phi}, \tag{1}$$

where $\phi > 0$ and $|\lambda| \leq 1$ are two additional shape parameters. Here, $G(x) = G(x; \boldsymbol{\xi})$ is the parent cdf and $\boldsymbol{\xi}$ is its parameter vector. The ET-G reduces to the exp-G when $\lambda = 0$ and simplifies to the T-G when $\phi = 1$. The probability density function (pdf) of the ET-G has the form

$$f(x) = f(x;\phi,\lambda,\boldsymbol{\xi}) = \phi\, g(x)\,[1+\lambda-2\,\lambda\, G(x)]\, G(x)^{\phi-1}\,[1+\lambda-\lambda\, G(x)]^{\phi-1}\,, \quad (2)$$

where $g(x) = g(x;\boldsymbol{\xi})$ is the baseline pdf. Let X be a random variable with density (2).

Many distributions have been proposed using the ET-G framework. Merovci et al. (2017) pioneered the exponentiated transmuted exponential, exponentiated transmuted Weibull, and exponentiated transmuted generalized half-normal by taking the exponential, Weibull, and half-normal as parent distributions, respectively. Okereke (2019) defined the exponentiated transmuted Lindley distribution, Abbas et al. (2021) introduced the exponentiated transmuted length-biased exponential distribution, and Eze & Yahya (2025) pioneered the transmuted exponential–compound Weibull–gamma distribution.

The statistical properties of these ET-G generalized models, designed to enhance more flexibility, are based on the formulation by Merovci et al. (2017), which relies on a double linear combination of exp-G densities. However, this formulation exhibits critical limitations, as its power series expansions are not convergent for all parameter configurations. To address this, an alternative linear representation is introduced, ensuring convergence and superior computational performance. The rest of the paper unfolds as follows. Section 2 revisits the original approach, Section 3 develops the new formulation, Section 4 presents a numerical validation. Section 5 presents applications, and Section 6 describes some conclusions.

2. Old Linear Representation

A linear representation for the density of the ET-G was derived by Merovci et al. (2017) as

$$f(x) = \sum_{k=0}^{\infty} b_k\, \Pi_{k+\phi}(x), \quad (3)$$

where

$$b_k = \sum_{i=0}^{\infty} (-1)^k\, \lambda^i \binom{\phi}{i}\binom{i}{k},$$

and $\Pi_{k+\phi}(x)$ is the cdf of the exp-G with power parameter $k+\phi$. According to the authors, Expression (3) can be used for computing the ordinary and incomplete moments and generating function of X.

However, the linear representation in (3) is not convergent for all terms of the series expansion and, therefore, cannot be used to derive the statistical properties. Note that two infinite sums are involved: the outer sum in k, and the inner sum in i that defines the coefficients b_k. This limitation can be illustrated by truncating the expansion and analyzing its behavior numerically. In this context, both the main series and the sum of the coefficients b_k are truncated at a finite value N. The limiting representation can be expressed as

$$f(x) = \lim_{N\to\infty} \sum_{k=0}^{N} \tilde{b}_k \, \Pi_{k+\phi}(x),$$

where

$$\tilde{b}_k = \tilde{b}_k(N) = \sum_{i=0}^{N} (-1)^k \lambda^i \binom{\phi}{i} \binom{i}{k}.$$

In practice, it is approximated by the truncated version

$$f(x) \approx \sum_{k=0}^{N} \tilde{b}_k \, \Pi_{k+\phi}(x), \tag{4}$$

for N large. The numerical behavior of this approximation is shown in Table 1 (Section 4).

3. An Improved Linear Representation

We present a novel linear representation for the ET-G family, which provides a more efficient and convergent formulation than the earlier expansion. Thus, from Equation (1), $|\lambda \, G(x)/(1+\lambda)| < 1$. The binomial theorem holds

$$(x+a)^v = \sum_{k=0}^{\infty} \binom{v}{k} x^k a^{v-k} \,, \tag{5}$$

if $v \in \mathbb{R}$ and $|x/a| < 1$. So, applying (5) in Equation (1),

$$F(x) = \sum_{k=0}^{\infty} w_k \, G(x)^{\phi+k}, \tag{6}$$

where

$$w_k = w_k(\phi,\lambda) = (-\lambda)^k \, (1+\lambda)^{\phi-k} \binom{\phi}{k}.$$

By differentiating (6), we obtain

$$f(x) = \sum_{k=0}^{\infty} w_k \, \pi_{\phi+k}(x) \,, \ \phi + k > 0 \,, \tag{7}$$

where $\pi_{\phi+k}(x) = \mathrm{d}\,\Pi_{\phi+k}(x)/\mathrm{d}x$. Since $G(x)$ is the cdf of a probability law, we have $0 \leq G(x) \leq 1$ for all x. Therefore, the coefficient series $\sum_{k=0}^{\infty} w_k$ converges absolutely for all $\phi > 0$ and $\lambda \in [-1, 1)$. The ratio of consecutive coefficients satisfies

$$\frac{w_{k+1}}{w_k} = \frac{-\lambda}{1+\lambda} \cdot \frac{\phi - k}{k+1}.$$

Taking absolute values and the limit as $k \to \infty$ yields

$$\lim_{k\to\infty} \left| \frac{w_{k+1}}{w_k} \right| = \frac{|\lambda|}{1+\lambda}.$$

For $\lambda \in [-1, 1)$ we have $1+\lambda > 0$ and $\frac{|\lambda|}{1+\lambda} < 1$. Hence, by the ratio test, the series $\sum_{k=0}^{\infty} w_k$ converges absolutely.

The case $\lambda = -1$ is excluded because it makes the denominator $1+\lambda = 0$, which is undefined. This restriction is consistent with the parameter space of the ET-G family, where $|\lambda| \leq 1$ with the understanding that $\lambda = -1$ is a boundary point that does not yield a proper distribution. Under these conditions, Equation (7) provides a simpler and convergent linear representation for the ET-G pdf, which constitutes the main result of this section, as it resolves the convergence issues of the earlier formulation in Equation (3).

Notice also that under this new representation, the ET-G density remains expressed as an infinite linear combination of the exp-G baseline, similar to the structure defined by Merovci et al. (2017), a formulation that is particularly advantageous since many mathematical properties can be determined easily from those of the exp-G family.

Figures 1(a) and 1(b) illustrate the convergence behavior of the new expansion with respect to parameters ϕ and λ, as well as the convergence of the weights w_k (which now sum one). These plots visually confirm that the approximation accuracy improves as more terms are included in the series.

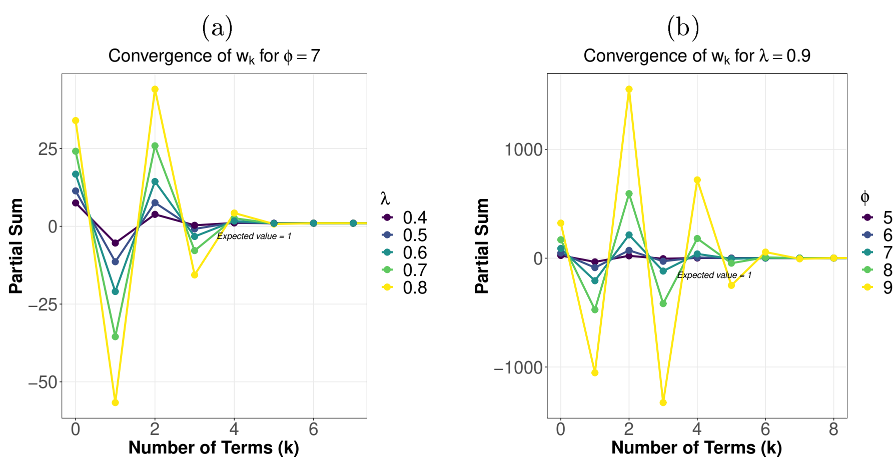

FIGURE 1: Convergence of partial sums of w_k for some values of λ and ϕ.

3.1. Moments and Generating Function

Let Y_k be a random variable with pdf $\pi_{\phi+k}(x)$. i.e., the exp-G density with power $\phi + k > 0$. We now present the moments, incomplete moments, and the generating function (gf) of the ET-G family.

Proposition 1. *By changing the sum in (7) with the integral in the definition of the expected value, we can easily obtain*

$$\mu_r' = \mathbb{E}(X^r) = \sum_{k=0}^{\infty} w_k \, \mathbb{E}\left(Y_k^r\right) \, .$$

Proposition 2. *The rth incomplete moment of X, say* $m_X^{(r)}(t) = \int_{-\infty}^{t} x^r \, f(x) \mathrm{d}x$, *can be expressed as a linear representation of exp-G incomplete moments, namely*

$$m_X^{(r)}(t) = \sum_{k=0}^{\infty} w_k \, m_{Y_k}^{(r)}(t),$$

where $m_{Y_k}^{(r)}(t) = \int_{-\infty}^{t} y^r \, \pi_{\phi+k}(y) \, dy$. *The proof is trivial.*

Proposition 3. *The generating function (gf) of X, say* $M_X(t) = \mathbb{E}[\mathrm{e}^{tX}]$, *is a linear combination of exp-G gfs, namely*

$$M_X(t) = \sum_{k=0}^{\infty} w_k \, M_{Y_k}(t),$$

where $M_{Y_k}(t) = \int_{-\infty}^{\infty} \mathrm{e}^{ty} \, \pi_{\phi+k}(y) \, dy$, *which is easily proved from Proposition 1.*

4. Numerical Study

To evaluate the convergence performance of the proposed series expansion for the ET-G family, we present a comparative analysis of both numerical integration and a pre-existing expansion, using the parent Weibull. So, the pdf and cdf of ET-Weibull (ET-W) can be expressed as

$$f(x; \phi, \lambda, \alpha, \beta) = \phi \, \alpha \, \beta^{-\alpha} x^{\alpha-1} \, \mathrm{e}^{-(x/\beta)^\alpha} \left[1 + \lambda - 2\left(1 - \mathrm{e}^{-(x/\beta)^\alpha}\right)\right] \times \left[1 - \mathrm{e}^{-(x/\beta)^\alpha}\right]^{\phi-1} \left[1 + \lambda - \lambda\left(1 - \mathrm{e}^{-(x/\beta)^\alpha}\right)\right]^{\phi-1} \, ,$$

and

$$F(x; \phi, \lambda, \alpha, \beta) = \left[1 - \mathrm{e}^{-(x/\beta)^\alpha}\right]^{\phi} \left[1 + \lambda - \lambda\left(1 - \mathrm{e}^{-(x/\beta)^\alpha}\right)\right]^{\phi},$$

respectively.

The moment expressions can be determined from the new expansion (for $r > -\alpha$) as

$$\mu_r' = \beta^r \, \Gamma\left(\frac{r}{\alpha} + 1\right) \sum_{k=0}^{\infty} w_k(\phi + k) \sum_{j=0}^{\infty} \frac{(-1)^j \binom{\phi+k-1}{j}}{(j+1)^{r/\alpha+1}} \,,$$

where $\Gamma(\cdot)$ is the gamma function. The reference for this comparison is the direct numerical integration (NI) of the moment given by

$$\mathbb{E}(X^r) = \phi\,\alpha\,\beta^{-\alpha} \int_0^{\infty} x^{\alpha+r-1}\,\mathrm{e}^{-(x/\beta)^\alpha} \left[1 + \lambda - 2\left(1 - \mathrm{e}^{-(x/\beta)^\alpha}\right)\right] \times \left[1 - \mathrm{e}^{-(x/\beta)^\alpha}\right]^{\phi-1} \left[1 + \lambda - \lambda\left(1 - \mathrm{e}^{-(x/\beta)^\alpha}\right)\right]^{\phi-1} \mathrm{d}x \,.$$

Table 1 details the first three ordinary moments for various parameter sets $\boldsymbol{\theta} = (\phi, \lambda, \alpha, \beta)^\top$. The moments are computed for both the new and old expansions, truncated at $N = 10, 50$, and 350, and they are compared with their corresponding NI values. The largest truncation point, $N = 350$, is chosen specifically to illustrate scenarios, where the old expansion begins to diverge. The table also presents Monte Carlo simulations, which are obtained by generating 100,000 random samples of X (each of size $n = 200$). As this method produces identical results for both the new and old expansions, the column shown refers to the new expansion for conciseness.

The proposed expansion shows excellent convergence and high precision. In many scenarios, such as scenario 6, the calculated moments correspond precisely to the NI values, even at a low truncation point of $N = 10$. In other cases, such as scenario 2, the expansion converges quickly, producing values at $N = 50$ that are very close to the NI. This high accuracy is achieved at minimal computational cost, as evidenced by the consistently low computation times, which are generally less than 0.01 seconds.

In specific cases like scenario 4, achieving high precision requires a higher truncation point. While the initial moment (μ_1') at $N = 10$ (0.85708818) shows a notable gap compared to the NI value (0.98745846), the expansion proves its robust convergence. By increasing the truncation to $N = 350$, the result improves to 0.98240846, significantly narrowing the discrepancy. This underscores that the choice of an appropriate truncation point N is critical to guarantee the desired accuracy.

In contrast, the old expansion demonstrates inferior performance. Although it produces reasonable estimates for some parameter sets, it often becomes unstable and diverges in many others. For instance, in scenario 2, the old expansion provides a plausible estimate at $N = 10$ but then diverges dramatically at $N = 350$, yielding a value of 5.235715×10^{125} for μ_1'. Similarly, in scenario 4, where the new expansion converges reliably, the old expansion produces an erroneous value of 12591.97 at $N = 350$. Across all tested scenarios, the new expansion consistently remained stable and converged towards the correct numerical integration values. Furthermore, even in cases where both expansions converge, such as scenario 6, the new expansion's computation times are significantly shorter, establishing it as both more reliable and more efficient.

The convergence performance of the proposed series expansion is further evaluated using the parent gamma distribution. The pdf and cdf of the ET-gamma (ET-G) distribution are given by

$$\begin{aligned} f(x) =& \frac{\phi\,\beta^{-\alpha}}{\Gamma(\alpha)}\; x^{\alpha-1}\mathrm{e}^{-x/\beta}\left[1+\lambda-2\,\lambda\,\gamma_1\left(\alpha,\frac{x}{\beta}\right)\right]\left[\gamma_1\left(\alpha,\frac{x}{\beta}\right)\right]^{\phi-1} \\ &\times\left[1+\lambda-\lambda\,\gamma_1\left(\alpha,\frac{x}{\beta}\right)\right]^{\phi-1}, \end{aligned} \tag{8}$$

where $\gamma_1 = \gamma(\alpha, x)/\Gamma(\alpha)$, $\gamma(\cdot, \cdot)$ is the incomplete gamma function and

$$F(x) = \left[\gamma_1\left(\alpha,\frac{x}{\beta}\right)\right]^{\phi}\left[1+\lambda-\lambda\,\gamma_1\left(\alpha,\frac{x}{\beta}\right)\right]^{\phi}.$$

The same approach applied in ET-W is used in ET-G, namely computing moments via numerical integration of (8) and comparing them with those obtained from expansions (4) and (7) of the exponentiated gamma. Table 2 presents the first three ordinary moments for various parameter sets $\boldsymbol{\theta} = (\phi, \lambda, a, b)^\top$. The results confirm the excellent convergence and stability of the proposed expansion, mirroring the findings observed for the ET-Weibull distribution. In all scenarios, the new expansion consistently converges to the numerical integration (NI) values, often achieving high precision even at low truncation points ($N = 10$ or $N = 50$). For instance, in scenarios 1 and 5, the moments calculated by the new expansion are virtually identical to the NI values across all truncation points. Conversely, the old expansion exhibits significant instability and divergence in several scenarios, such as 2, 3, and 4, particularly at higher truncation points ($N = 350$), where it yields erroneous or extremely large values. This comparative analysis strongly validates the superior performance, reliability, and computational efficiency of the new series expansion for the ET-gamma distribution. The `R` scripts used to obtain the results are available at the link `https://github.com/alexaaf31/ET-G-family-`.

TABLE 1: Comparison of the results from the new and old expansions for the ET-Weibull, under different scenarios, values of N, convergence times, Monte Carlo, and NI.

Scenario	$\boldsymbol{\theta}$	Moment	$N = 10$ New	$N = 10$ Old	$N = 50$ New	$N = 50$ Old	$N = 350$ New	$N = 350$ Old	Monte Carlo	NI
1	(0.5, 0.1, 1.9, 3.4)	μ'_1	1.9738	1.9738	2.0308	2.0308	2.0440	2.0440	2.0463	2.0461
		Time (s)	< 0.01	0.03	< 0.01	0.03	0.02	0.12	–	–
		μ'_2	6.7343	6.7343	6.7814	6.7814	6.7861	6.7861	6.7881	6.7863
		Time (s)	< 0.01	0.05	0.02	0.01	< 0.01	0.13	–	–
		μ'_3	28.9329	28.9329	28.9810	28.9810	28.9832	28.9832	28.9968	28.9832
		Time (s)	< 0.01	0.06	< 0.01	0.03	0.02	0.14	–	–
2	(2.5, 0.9, 1.9, 3.4)	μ'_1	3.0807	3.0804	3.0870	3.0234	3.0870	5.2357e+125	3.0871	3.0870887
		Time (s)	< 0.01	0.02	< 0.01	0.01	0.01	0.11	–	–
		μ'_2	10.9204	10.9200	10.9262	10.9728	10.9263	1.7886e+125	10.9268	10.9263
		Time (s)	< 0.01	0.02	< 0.01	0.03	0.01	0.12	–	–
		μ'_3	43.6764	43.6753	43.6826	43.7455	43.6826	7.8098e+124	43.6830	43.6826
		Time (s)	< 0.01	0.03	< 0.01	0.02	0.02	0.13	–	–
3	(1.5, 0.6, 1.9, 3.4)	μ'_1	2.9375	2.9375	2.9268	2.9268	2.9263	9.4703e+64	2.9262	2.9263
		Time (s)	< 0.01	0.01	< 0.01	0.03	0.02	0.12	–	–
		μ'_2	10.6339	10.6339	10.6243	10.6243	10.6241	5.0815e+64	10.6234	10.6241
		Time (s)	< 0.01	0.03	< 0.01	0.02	0.02	0.11	–	–
		μ'_3	45.7219	45.7220	45.7115	45.7115	45.7114	3.5682e+64	45.7032	45.7114
		Time (s)	< 0.01	0.02	< 0.01	0.03	0.02	0.11	–	–
4	(0.2, 0.4, 1.9, 3.4)	μ'_1	0.8570	0.8570	0.9438	0.9438	0.9824	12591.9700	0.9872	0.9874
		Time (s)	< 0.01	0.08	< 0.01	0.11	0.17	0.50	–	–
		μ'_2	2.5120	2.5120	2.5816	2.5816	2.5938	4348.9600	2.5935	2.5941
		Time (s)	< 0.01	0.03	0.01	0.08	0.27	0.45	–	–
		μ'_3	9.6878	9.6878	9.7575	9.7575	9.7626	1794.7450	9.7636	9.7626
		Time (s)	< 0.01	0.14	0.01	0.19	0.17	0.27	–	–
5	(0.2, 0.8, 1.9, 3.4)	μ'_1	0.7168	0.7171	0.8081	0.8366	0.8426	2.0671e+113	0.8539	0.8540
		Time (s)	< 0.01	0.07	0.01	0.40	0.10	0.39	–	–
		μ'_2	1.8376	1.8377	1.9107	1.9178	1.9227	6.7455e+112	1.9235	1.9238
		Time (s)	< 0.01	0.12	0.01	0.08	0.08	0.50	–	–
		μ'_3	6.1505	6.1496	6.2224	6.2294	6.2277	2.6160e+112	6.2272	6.2278
		Time (s)	0.01	0.08	0.02	0.12	0.22	0.62	–	–
6	(3.0, 0.7, 1.9, 3.4)	μ'_1	3.5724	3.5724	3.5724	3.5724	3.5724	3.5724	3.5727	3.5724
		Time (s)	< 0.01	0.15	< 0.01	0.17	0.03	0.45	–	–
		μ'_2	14.5475	14.5475	14.5475	14.5475	14.5475	14.5475	14.5502	14.5475
		Time (s)	< 0.01	0.10	< 0.01	0.14	0.02	0.30	–	–
		μ'_3	66.7335	66.7335	66.7335	66.7335	66.7335	66.7335	66.7564	66.7335
		Time (s)	< 0.01	0.11	< 0.01	0.09	0.03	0.32	–	–
7	(3.5, 0.5, 1.9, 3.4)	μ'_1	4.0375	4.0375	4.0355	4.0355	4.0355	7.8643e+34	4.0357	4.0355
		Time (s)	< 0.01	0.15	0.01	0.11	0.06	0.55	–	–
		μ'_2	18.2875	18.2875	18.2855	18.2855	18.2855	2.5810e+34	18.2879	18.2855
		Time (s)	0.02	0.17	< 0.01	0.14	0.04	0.61	–	–
		μ'_3	92.0097	92.0097	92.0074	92.0074	92.0074	1.0474e+34	92.0254	92.0074
		Time (s)	< 0.01	0.20	< 0.01	0.26	0.03	0.44	–	–
8	(4.0, 0.2, 1.9, 3.4)	μ'_1	4.5868	4.5868	4.5868	4.5868	4.5868	4.5868	4.587183	4.5868
		Time (s)	< 0.01	0.14	< 0.01	0.14	0.01	0.42	–	–
		μ'_2	23.1181	23.1181	23.1181	23.1181	23.1181	23.1181	23.1216	23.1181
		Time (s)	0.03	0.16	< 0.01	0.15	0.01	0.47	–	–
		μ'_3	126.8847	126.8848	126.8847	126.8848	126.8847	126.8848	126.9157	126.8847
		Time (s)	< 0.01	0.18	0.01	0.26	0.02	0.36	–	–

Table 2: Comparison of the results from the new and old expansions for the ET-gamma, under different scenarios, values of N, convergence times, Monte Carlo, and NI.

Scenario	$\boldsymbol{\theta}$	Moment	$N = 10$ New	$N = 10$ Old	$N = 50$ New	$N = 50$ Old	$N = 350$ New	$N = 350$ Old	Monte Carlo	NI
1	$(1.9, 0.1, 1.3, 2.4)$	μ_1'	4.2331	4.2331	4.2331	4.2331	4.2331	4.2331	4.2335	4.2331
		Time (s)	0.01	0.03	0.01	0.04	0.01	0.05	–	–
		μ_2'	26.4137	26.4137	26.4137	26.4137	26.4137	26.4137	26.4213	26.4137
		Time (s)	0.01	0.02	0.02	0.05	0.02	0.43	–	–
		μ_3'	221.1638	221.1638	221.1638	221.1638	221.1638	221.1638	221.2967	221.1638
		Time (s)	0.02	0.02	0.02	0.06	< 0.01	0.46	–	–
2	$(2.9, 0.9, 1.3, 2.4)$	μ_1'	3.2027	3.20273	3.2027	3.2027	3.2027	-3.1381e+66	3.2028	3.2027
		Time (s)	0.02	0.03	0.04	0.07	0.01	0.45	–	–
		μ_2'	14.1368	14.1367	14.1367	14.1367	14.1367	-1.3705e+68	14.1357	14.1362
		Time (s)	0.01	0.01	0.03	0.06	0.02	0.47	–	–
		μ_3'	84.3255	84.3248	84.3248	83.8763	84.3248	-7.6316e+69	84.2883	84.3259
		Time (s)	0.01	0.03	0.01	0.08	0.03	0.49	–	–
3	$(1.2, 0.8, 1.3, 2.4)$	μ_1'	2.2223	2.2223	2.2223	2.2223	2.2223	2.2314e+52	2.2222	2.2223
		Time (s)	0.02	0.03	0.03	0.08	0.03	0.45	–	–
		μ_2'	8.7230	8.7232	8.7232	8.723	8.7232	4.9326e+53	8.7201	8.7232
		Time (s)	0.02	0.04	0.02	0.07	0.04	0.46	–	–
		μ_3'	52.4538	52.4552	52.4552	54.2205	52.4552	1.8400e+55	52.3834	52.4552
		Time (s)	0.02	0.04	0.02	0.06	0.02	0.45	–	–
4	$(0.2, 0.8, 1.3, 2.4)$	μ_1'	0.6107	0.6108	0.6107	0.6107	0.6107	-6.2142e+54	0.6106	0.6107
		Time (s)	0.01	0.04	0.03	0.06	0.03	0.50	–	–
		μ_2'	1.7646	1.7642	1.7641	1.7641	1.7641	-8.9262e+55	1.7648	1.7641
		Time (s)	< 0.01	0.03	0.03	0.06	0.05	0.47	–	–
		μ_3'	9.4517	9.4462	9.4461	152.4932	9.4461	-2.6951e+56	9.4599	9.4461
		Time (s)	0.01	0.03	0.03	0.06	0.03	0.45	–	–
5	$(5.0, 0.1, 1.3, 2.4)$	μ_1'	6.4078	6.4078	6.4078	6.4078	6.4078	6.4078	6.4078	6.4078
		Time (s)	< 0.01	0.03	0.01	0.06	0.02	0.46	–	–
		μ_2'	50.7690	50.7690	50.7690	50.7690	50.7690	50.7690	50.7662	50.7690
		Time (s)	0.02	0.03	< 0.01	0.08	0.02	0.42	–	–
		μ_3'	488.0425	488.0426	488.0425	488.0426	488.0425	488.0426	488.0001	488.0426
		Time (s)	0.02	0.03	< 0.01	0.06	0.01	0.45	–	–
6	$(2.5, 0.7, 1.3, 2.4)$	μ_1'	3.4980	3.4980	3.4980	3.4980	3.4980	-6.8108e+29	3.4986	3.4980
		Time (s)	0.01	0.04	0.03	0.08	0.03	0.45	–	–
		μ_2'	17.9120	17.9120	17.9120	17.9120	17.9120	-4.3802e+31	17.9202	17.9118
		Time (s)	0.01	0.03	0.02	0.06	0.03	0.44	–	–
		μ_3'	127.6748	127.6744	127.6744	127.6745	127.6744	-2.6413e+33	127.8112	127.6749
		Time (s)	0.01	0.01	0.02	0.06	0.02	0.45	–	–
7	$(0.5, 0.5, 1.3, 2.4)$	μ_1'	1.5187	1.5187	1.5187	1.5187	1.5187	1.5187	1.5190	1.5187
		Time (s)	0.02	0.02	0.01	0.06	0.02	0.45	–	–
		μ_2'	6.1055	6.1055	6.1055	6.1055	6.1055	6.1055	6.1078	6.1055
		Time (s)	0.02	0.01	0.02	0.06	0.02	0.45	–	–
		μ_3'	40.9632	40.9629	40.9629	40.9629	92.0074	40.9629	40.9654	40.9629
		Time (s)	0.03	0.04	0.03	0.08	0.02	0.44	–	–
8	$(0.1, 0.1, 1.3, 2.4)$	μ_1'	0.4939	0.4939	0.4939	0.4939	0.4939	0.4939	0.4942	0.4939
		Time (s)	0.01	0.01	0.02	0.06	0.01	0.48	–	–
		μ_2'	1.9508	1.9508	1.9508	1.9508	1.9508	1.9508	1.9534	1.9508
		Time (s)	0.01	0.03	0.01	0.07	0.02	0.47	–	–
		μ_3'	13.6326	13.6326	13.6326	13.6326	13.6326	13.6326	13.6551	13.6326
		Time (s)	0.02	0.03	0.02	0.08	< 0.01	0.47	–	–

5. Application

To evaluate the importance of the ET-G family of distributions, this study utilizes a real-world data set from the field of bibliometrics. The data are sourced from Thomson Reuters Journal Citation Reports (JCR) platform. The analysis centers on the "Citations / Doc. (2 years)" indicator, a standard metric reflecting the average number of citations received in a specific year by articles published over the preceding two years. Edition 2024, which is the last available. This metric is employed as a proxy for a journal's contemporary impact and scholarly influence. Similar bibliometric indicators have been modeled statistically in previous studies, underscoring the relevance of distributional approaches in this context (Peña-Ramírez et al., 2020). The data set comprises 282 journals, all of which are formally categorized under the "Probability and Statistics" field.

TABLE 3: Results for journal citation data.

Model	MLEs (SEs)			
ET-W $(\alpha, \beta, \phi, \lambda)$	0.870	1.462	2.711	0.828
	(0.123)	(0.300)	(0.025)	(0.119)
Exp-W $(\alpha, \beta, \phi, 0)$	4.207	0.667	0.465	–
	(1.494)	(0.097)	(0.746)	–
T-W $(\alpha, \beta, 1, \lambda)$	1.347	2.471	0.746	–
	(0.058)	(0.178)	(0.108)	–
WE$(\alpha, \beta, 1, 0)$	0.576	1.234	–	–
	(0.029)	(0.053)	–	–

Table 3 presents the maximum likelihood estimates (MLEs) and their corresponding standard errors (SEs) for the fitted models were obtained using the AdequacyModel package (Marinho et al., 2019) in the statistical software R (R Core Team, 2024), employing the Broyden–Fletcher–Goldfarb–Shanno (BFGS) optimization algorithm. The results for the ET-W, Exp-W, T-W and Weibull (WE) distributions were found to be accurate.

The results in Table 4 demonstrate that the ET-W distribution outperforms the other distributions, as evidenced by its lower values of Cramér-von Mises statistic (W^*), Anderson-Darling statistic (A^*), Akaike information criterion (AIC), consistent Akaike information criterion (CAIC), Bayesian information criterion (BIC), Hannan-Quinn information criterion (HQIC), and Kolmogorov-Smirnov (KS) with its corresponding p-value. Figure 2 shows that the estimated pdf and cdf of the ET-W distribution are closer to the histogram and the empirical cdf, respectively. These findings suggest that the ET-W distribution provides the best fit for these data.

TABLE 4: Adequacy measures for journal citation data.

Model	W^*	A^*	AIC	CAIC	BIC	HQIC	KS	p-value
ET-W	0.121	0.748	782.569	782.715	797.094	788.396	0.048	0.518
Exp-W	0.159	0.971	783.283	783.370	794.176	787.653	0.056	0.345
T-W	0.273	1.759	795.559	795.646	806.453	799.929	0.070	0.127
WE	0.411	2.595	806.669	806.713	813.932	809.583	0.088	0.024

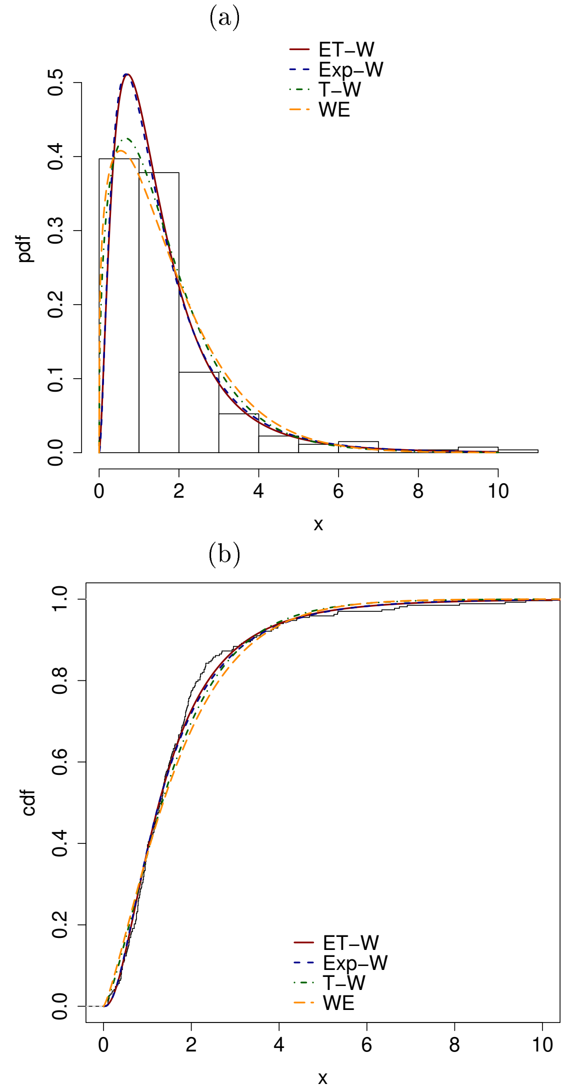

Figure 2: Journal citation data: (a) Estimated pdfs. (b) Estimated cdfs.

Table 5: Comparison of the first three ordinary moments of ET-Weibull obtained by series expansions (new and old) and NI.

Moment	$N = 10$		$N = 50$		$N = 350$		NI
	New	Old	New	Old	New	Old	
$\hat{\mu}'_1$	1.6023	1.6023	1.6027	1.6028	1.6027	1.9859e+112	1.6027
$\hat{\mu}'_2$	4.5962	4.5961	4.5962	4.5962	4.5962	2.9032e+110	4.5962
$\hat{\mu}'_3$	21.6314	21.6311	21.6311	21.6311	21.6311	6.8592e+108	21.6311

Table 5 presents a comparative analysis of the first three estimates of the ordinary moments ($\hat{\mu}'_1$, $\hat{\mu}'_2$, $\hat{\mu}'_3$) for the ET-Weibull distribution and serves as numerical validation of the new series expansion in relation to the old formulation. The statistical focus lies on the accurate estimation of the distribution moments, which is essential for characterizing probability laws through mean, variance, skewness, and kurtosis. The academic importance stems from demonstrating the superior convergence and stability of the new method, especially under conditions where the old one fails catastrophically.

For the new expansion, the estimated moments ($\hat{\mu}'_1 \approx 1.6027$, $\hat{\mu}'_2 \approx 4.5962$, $\hat{\mu}'_3 \approx 21.6311$) remain consistent between truncation points ($N = 10, 50, 350$), converging rapidly to the NI benchmark. This fast and stable convergence, even at $N = 10$, confirms that the new linear representation, based on a single sum, solves the convergence problems inherent in the old formulation. In contrast, the old expansion shows severe instability and divergence as N increases. Although the results at $N = 10$ and $N = 50$ appear plausible, the values at $N = 350$ explode to high values (e.g., $\hat{\mu}'_1 \approx 1.9859e + 112$), exposing a critical flaw in the power series expansion. Thus, the table provides definitive empirical evidence that the new, simpler linear representation is not merely an alternative, but a necessary methodological improvement for the accurate and general calculation of statistical properties in the ET-G family.

6. Concluding Remarks

A significant deficiency in the linear representation of the exponentiated transmuted-G (ET-G) family of distributions was addressed. The original expansion, based on a power series, was shown to fail to converge for all parameter settings, rendering its derived statistical properties unreliable. To resolve this issue, a new and mathematically rigorous linear representation was proposed and derived. A numerical investigation, using the Weibull distribution as a baseline, compared this new expansion with the previous formulation and with direct numerical integration. The results clearly indicated that the newly proposed formulation was stable and converged accurately across all tested cases. In contrast, the earlier expansion exhibited instability, often failing to converge or diverging in critical scenarios. This work thus established a reliable and computationally efficient framework for analyzing and applying the ET-G family.

[Received: September 2025 — Accepted: November 2025]

References

Abbas, S., Mohsin, M. & Pilz, J. (2021), ‘A new lifetime distribution with applications in reliability and environmental sciences’, *Journal of Statistics and Management Systems* **24**(3), 453–479.

Alrweili, H. (2025), ‘Statistical inference and data analysis of the record-based transmuted Burr X model’, *Open Mathematics* **23**(1), 20240121.

Aryal, G. R. & Tsokos, C. P. (2011), 'Transmuted Weibull distribution: A generalization of the Weibull probability distribution', *European Journal of pure and applied mathematics* **4**(2), 89–102.

Bashiru, S. O., Kayid, M., Sayed, R., Balogun, O. S., Hammad, A. & Abd El-Raouf, M. (2025), 'Transmuted inverse unit Teissier distribution: Properties, estimations and applications to medical and radiation sciences', *Journal of Radiation Research and Applied Sciences* **18**(1), 101208.

Cogo, C. C., de Andrade, T. A. N. & Bisognin, C. (2024), 'New unconditional and quantile regression model erf-Weibull: An alternative to gamma, Gumbel and exponentiated exponential distributions', *Revista Colombiana de Estadística* **47**(2), 301–327.

Cordeiro, G. M. & de Castro, M. (2011), 'A new family of generalized distributions', *Journal of Statistical Computation and Simulation* **81**, 883–898.

Debastiani Neto, J., Puziol de Oliveira, R., Antonio Moala, F. & Alberto Achcar, J. (2025), 'Introducing the discrete xLindley distribution: A one-parameter model for overdispersed data', *Revista Colombiana de Estadística* **48**(1), 39–70.

Dey, S., Raheem, E. & Mukherjee, S. (2017), 'Statistical properties and different methods of estimation of transmuted Rayleigh distribution', *Revista Colombiana de Estadística* **40**(1), 165–203.

Eugene, N., Lee, C. & Famoye, F. (2002), 'Beta-normal distribution and its applications', *Communications in Statistics - Theory and Methods* **31**, 497–512.

Eze, N. M. & Yahya, W. B. (2025), 'Bayesian and non-Bayesian reliability analysis with a new member of transmuted exponential-G family of distribution', *Journal of Statistical Computation and Simulation* pp. 1–44.

Ferreira, A. A. & Cordeiro, G. M. (2024), 'The flexible generalized gamma distribution with applications to COVID-19 data', *Revista Colombiana de Estadística* **47**(2), 453–473.

Gupta, R. C., Gupta, P. L. & Gupta, R. D. (1998), 'Modeling failure time data by Lehman alternatives', *Commun. Stat. Theory Methods* **27**(4), 887–904.

Khan, M. S. & King, R. (2013), 'Transmuted modified Weibull distribution: A generalization of the modified Weibull probability distribution', *European Journal of pure and applied mathematics* **6**(1), 66–88.

Lehmann, E. L. (1953), 'The power of rank tests', *Annals of Mathematical Statistics* **24**, 23–43.

Marinho, P. R. D., Silva, R. B., Bourguignon, M., Cordeiro, G. M. & Nadarajah, S. (2019), 'AdequacyModel: An R package for probability distributions and general purpose optimization', *PLoS One* **14**(8).

Merovci, F., Alizadeh, M., Yousof, H. M. & Hamedani, G. G. (2017), 'The exponentiated transmuted-G family of distributions: Theory and applications', *Commun. Stat. Theory Methods* **46**(21), 10800–10822.

Mota, A. L., Ramos, P. L., Ferreira, P. H., Tomazella, V. L. & Louzada, F. (2021), 'A reparameterized weighted Lindley distribution: properties, estimation and applications', *Revista Colombiana de Estadística* **44**(1), 65–90.

Okereke, E. W. (2019), 'Exponentiated transmuted Lindley distribution with applications', *Open J. Math. Anal.* **3**(2), 1–18.

Peña-Ramírez, F. A., Guerra, R. R., Canterle, D. R. & Cordeiro, G. M. (2020), 'The logistic Nadarajah–Haghighi distribution and its associated regression model for reliability applications', *Reliability Engineering & System Safety* **204**, 107196.

R Core Team (2024), *R: A Language and Environment for Statistical Computing*, R Foundation for Statistical Computing, Vienna, Austria. https://www.R-project.org/

Shahzad, M. N., Merovci, F. & Asghar, Z. (2017), 'Transmuted Singh-Maddala distribution: A new flexible and upside-down bathtub shaped hazard function distribution', *Revista Colombiana de Estadística* **40**, 1–27.

Shaw, W. T. & Buckley, I. R. C. (2007), 'The alchemy of probability distributions: beyond Gram-Charlier expansions, and a skew-kurtotic-normal distribution from a rank transmutation map', *arXiv preprint arXiv:0901.0434* .